Viscoelastic Characteristics of Shape Memory Polymers

Zhengdao Wang, Zhengfa Li, Linyun Wang, Zhiyuan Xiong, Wang Zhengdao, Zhengfa Li, Linyun Wang, Zhiyuan Xiong

Department of Mechanics, School of Civil Engineering, Beijing Jiao-Tong University, Beijing 100044, China

Received 15 October 2009; accepted 5 March 2010
DOI 10.1002/app.32420
Published online 3 June 2010 in Wiley InterScience (www.interscience.wiley.com).

ABSTRACT: Shape memory polymers (SMPs) can keep a temporary state and subsequently recover to the original shape through a prescribed thermomechanical process. Although different theoretical models have been presented, the viscous effects were seldom considered. This article aims to provide an insight into the viscoelastic property of SMPs and its effect on the functional realization. Systematic thermomechanical experiments were performed. Special considerations were focused on the viscoelastic response of SMPs in the vicinity of the glass transition temperature T_g. The relations between shape switching transition temperature T_{tran} and T_g were also discussed. The results confirm that T_{tran} departs from T_g due to the viscoelastic effect and does not keep a constant value during heating and cooling processes. The viscoelastic effect reaches to maximum value at T_g, then decreases slowly at cooling and quickly at heating.
© 2010 Wiley Periodicals, Inc. J Appl Polym Sci 118: 1406–1413, 2010

Key words: shape memory polymer; critical transition temperature; thermomechanics; viscoelasticity

INTRODUCTION

Shape memory polymers (SMPs) are a new class of functional materials. Compared with the traditional shape memory alloys and ceramics, SMPs own some unique advantages, e.g., low density (1.1–1.3 g/cm^3), high frozen strain (up to 400%), low manufacturing cost, easy processing, wide shape transition temperature, and even biocompatibility.[1] Besides the initial application as heat-shrinkable tubes,[2] SMPs have nearly spanned various areas of our life. For example, degradable SMPs have been applied in the construction of hematology-related products and devices.[3–5] SMP-based composites reinforced by continuous fibers have received great interest in the future deployable industry.[6–8] SMP-based micro-actuators (e.g., micro-pumps and micro-valves) can be integrated into the soft-lithography fabrication methodology with minimal process modification.[9–11]

Although some new stimulus conditions, e.g., electrical current and moisture,[12,13] have been investigated, heating stimulus is still the primary selection for SMPs to realize their shape memory functionality. Generally, a shape frozen/recovery thermomechanical cycle of SMPs consists of the following steps: (a) deforming the specimens at an elevated temperature; (b) keeping such deformation and decreasing the temperature to be lower than a switching transition value T_{tran}, which causes the deformed shape to be "frozen" even if unloading; (c) recovering the original shape by increasing the temperature to be higher than T_{tran}.

In the last decade, various new SMPs and SMP-based composites were reported.[14–20] In another aspect, experimental and theoretical studies of the thermomechanical behavior of SMPs also received great attention. In a review article, Lendlein and Kelch[21] discussed the molecular deformation mechanism and thermomechanical properties of SMPs in details. Tobushi et al.[22,23] performed a series of thermomechanical experiments of shape memory polyurethanes and simulated the shape memory effect by introducing a slip element into the traditional viscoelastic models of polymers. Rao et al.[24] delineated the modeling of SMPs into four parts and addressed these parts separately by using a framework that was developed for studying the crystallization behavior of polymers.[25] Abrahamson et al.[26] proposed a lumped-parameter model to correlate the different responses of SMPs at temperatures spanning glassy and rubbery states. Liu et al.[27] developed a small-strain constitutive model which can effectively describe their test results. Recently, Chen et al.[28] proposed a 3-D, large-deformation thermomechanical model. Wang et al.[29] presented a new constitutive model with consideration of the frozen retardant time and the difference between thermal and mechanical frozen fractions.

Although extensive work has been performed on the thermomechanical behavior of SMPs, some issues remain unresolved. For example, as a class of semi-crystallized polymers, SMPs might exhibit

Correspondence to: Z. Wang (zhdwang@bjtu.edu.cn).
Contract grant sponsor: Natural Science Foundations of China; contract grant number: 10872025.
Contract grant sponsor: Ministry of Education of the People's Republic of China (NECT) and the Fundamental Research Funds for the Central Universities.

© 2010 Wiley Periodicals, Inc.

Figure 1 Thermomechanical testing device of SMPs. [Color figure can be viewed in the online issue, which is available at www.interscience.wiley.com.]

viscoelastic response in the vicinity of T_g. However, until now most thermomechanical constitutive equations about SMPs are rate-independent. Moreover, a parameter, T_{tran}, which denotes the shape switching transition temperature between the frozen and recovery states, was commonly introduced in many theoretical models. It is known that T_g is defined as the critical glass transition temperature of polymers. Then how about the relations between T_{tran} and T_g? The present article aims to provide some experimental results and theoretical analysis about these issues, which should be of benefit to understanding of the deformation mechanisms of SMPs and can also provide some clues in deriving rate-related thermomechanical constitutive equations for this class of functional materials.

TESTING RESULTS AND THEORETICAL ANALYSIS

Materials and specimens

Test specimens were prepared from a type of commercial shape-memory polyurethane, supplied by Composite Technology Development (CTD), Incorporated. The size of the specimens is 50 × 15 × 3.34 mm^3 (length × width × thickness). Systematic thermomechanical experiments were performed in this study, which includes the shape frozen and recovery tests under different constraint conditions, thermal strain test under free state, tensile stress-strain hysteresis and stress relaxation tests under different loading rates and different temperatures. All experiments were performed by a Zwich-5000 testing system and a temperature-controlled environmental chamber (see Fig. 1). The temperature range is 293–353 K (20–80°C), which spans the glassy transition temperature of the material (about 326 K). The temperature was measured by the thermocouple thermometer.

A few thermal cycles were carried out before experiments, which can effectively eliminate the prefrozen strain accumulated during the fabrication process and receive more stable experimental data. To realize temperature equilibrium in specimens, the heating/cooling rate was selected to be ±0.5 K/min.

Thermal strain and coefficient of thermal expansion

Figure 2(a) presents the experimental curve of thermal strain versus temperatures in the range of 293–353 K. The coefficient of thermal expansion (CTE) is defined as the slope of the thermal strain curve.

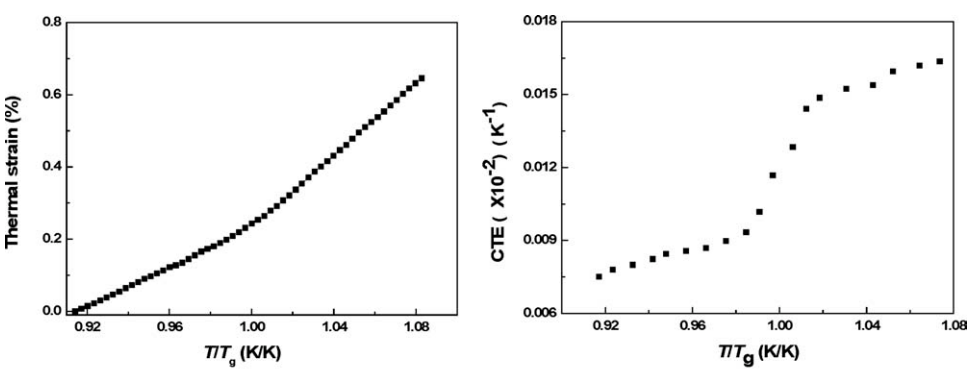

(a) thermal strain (b) coefficient of thermal expansion

Figure 2 Thermal strain and coefficient of thermal expansion as functions of the temperature.

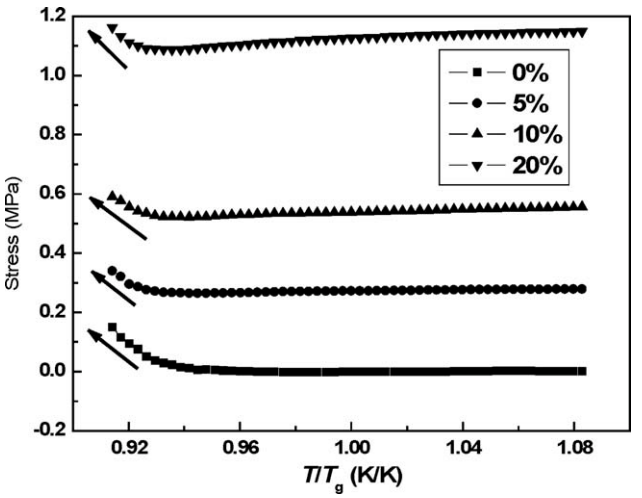

Figure 3 Stress responses during the cooling process under different prestrain constraint conditions.

After smoothing the thermal strain curve, CTE was received by differentiating the thermal strain data by temperatures. The results are shown in Figure 2(b). Compared with the thermal strain, CTE testing results provide more information about the microstructures of the material. Nearly linear relations exist between CTE and the temperature when the material is in either glassy or rubbery state. However, a significant change of CTE-values exhibits in the vicinity of the T_g (~326 K), which reflects the change of the free-volume fraction during the glass transition zone of the material. Thus, the curve of CTE versus temperature clearly reflects the different micro-structure characteristics of the material in glassy and rubbery states.

Shape frozen response

The thermomechanical cycle of SMPs used in applications often involves two processes: frozen response during the cooling process under a predesigned constant strain and recovery response during the heating process under free or constraint conditions. Figure 3 provides testing results of frozen responses of shape-memory polyurethane under different constraint conditions. During the cooling process under higher constant-strain conditions (e.g., 20% of prestrain), the stress keeps slowly decreasing until the temperature is much lower than T_g. When the temperature is close to a shape switching transition temperature T_{tran}, the stress inversely increases quickly (see the arrows shown in Fig. 3). With decreasing of the prestrains, the declining rate of the stress versus T/T_g before the transition point is slightly decreased while T_{tran}. In addition, different from CTE testing results, T_{tran} seems to be obviously apart from T_g of the material during the cooling process. To be clearer, Figure 4(a) presents the declining rates of the stresses versus temperatures in the stage of the testing temperature to be higher than T_{tran}. Figure 4(b) shows the normalized switching transition temperatures under different constraint conditions, which are determined by the conversion points of the stresses from decreasing to increasing. The results show that a higher prestrain will accelerate the stress relaxation at the first stage and decrease the shape switching transition of the material during the cooling process.

The above phenomena might be caused by the viscous effect of the material near the glassy transition zone. Figure 5 shows the typical curves of the storage modulus, loss modulus, and tan delta of most polymers versus testing temperatures. The viscoelastic characteristics reach to maximum values at T_g. SMPs should have the similar viscoelastic properties with other polymeric materials. For SMPs under constant strain conditions during the cooling process, thermal shrinking will cause a stress accumulation, but strain frozen and stress relaxation will reversely decrease the stress level. A higher strain-constraint condition leads to a larger frozen strain and a higher stress relaxation rate. Hence, the declining rate of the stress in that case is higher than that at the lower prestrain level.

In addition, during the frozen process on the condition of constant strain-constraints, the significant viscoelastic effect in the glassy transition zone will delay the shape transition process and cause T_{tran} to

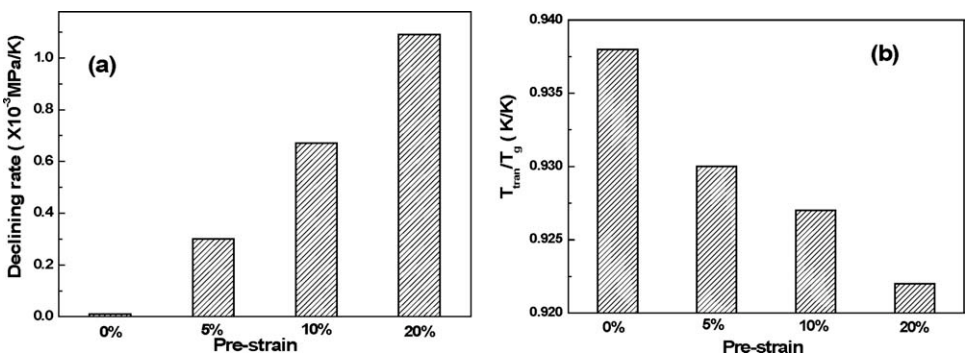

Figure 4 Prestrain effect on the shape frozen response of shape-memory polyurethane.

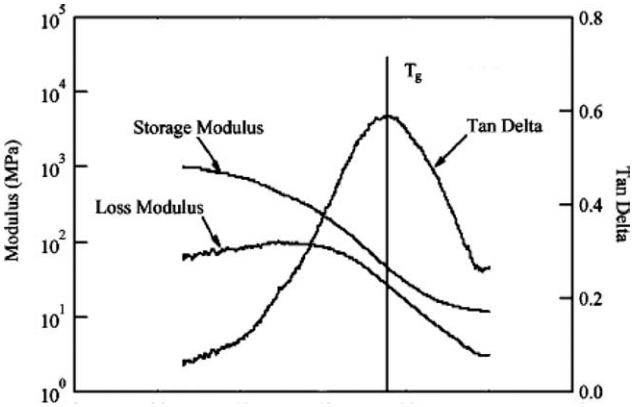

Figure 5 Typical storage modulus, loss modulus, and tan delta of polymers.

be apart from T_g. The stress level does not increase until the testing temperature is much lower than T_g, where viscoelastic effect can be neglected and thermal stress accumulation becomes a dominate role. Comparatively, CTE test is on the condition of a free state. Thus the transition temperature is very close to T_g.

Figure 6 shows the experimental results of the Young's modulus affected by temperatures. Since the Young's modulus of shape-memory polyurethane in the glassy state is about two-order higher than that in the rubbery state, the stress increases very quickly when the temperature is lower than T_{tran} during the cooling process.

Shape recovery response

The condition of the shape recovery of SMPs is more complex than that of the shape frozen. In addition to free strain recovery, some flexible constraints are commonly under considerations for meeting different application requirements. For example, in a minimally invasive surgical application, the precompacted SMP is subjected to a flexible constraint from

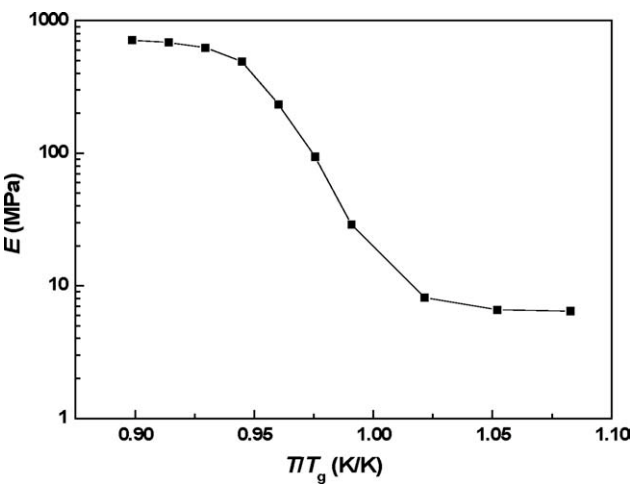

Figure 6 Young's modulus versus testing temperatures.

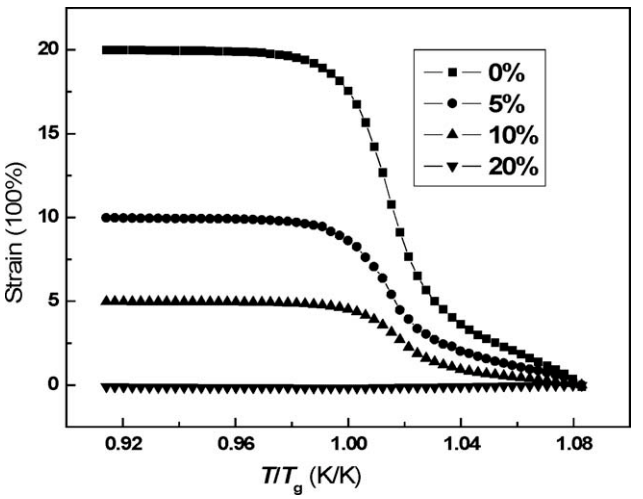

Figure 7 Free-recovery responses during the heating process.

the surrounding tissue during the recovery process.[30] In contrast, when a prestretched suture is used to close a skin laceration, a reactive tensile stress is generated.[31] Hence, the corresponding thermomechancial responses must be considered.

Figure 7 shows the free-recovery strain response of the shape memory polyurethane during heating. It is clear that the frozen strain keeps a nearly constant value until the testing temperature is very close to T_g. Above T_g, the strain-recovery paths under different prestrains are similar, and all specimens quickly recover to their original shapes. If we define T_{tran} by the maximum slope of the strain recovery, the value during the heating process is very close to T_g. One reason is that no external load is applied during the free-recovery process. Naturally viscoelasticity plays less contribution than that during the constant-strain frozen process. Another reason might be that the viscoelastic contributions of SMPs at the rubbery and glassy states are different, which will be discussed in the following sections.

The constant strain-constraint and stress-constraint recovery responses are shown in Figures 8 and 9, respectively. On the condition of constant strain-constraint recovery response, the stress keeps nearly constant in the beginning and then increases very quickly due to the increase of the unfrozen strain. When the prestrain has been mostly recovered, the stress becomes stable. The final stresses on different conditions are almost fully recovered to the initial predeformation values. For the stress-constraint recovery response as shown in Figure 9, the strain recovery paths under different stress-constraints are similar. The final unrecovered strain levels are determined by the constraint stress and the Young's modulus of the material in rubbery state.

The above results confirm that the T_{tran}-values of SMPs during cooling and heating processes are

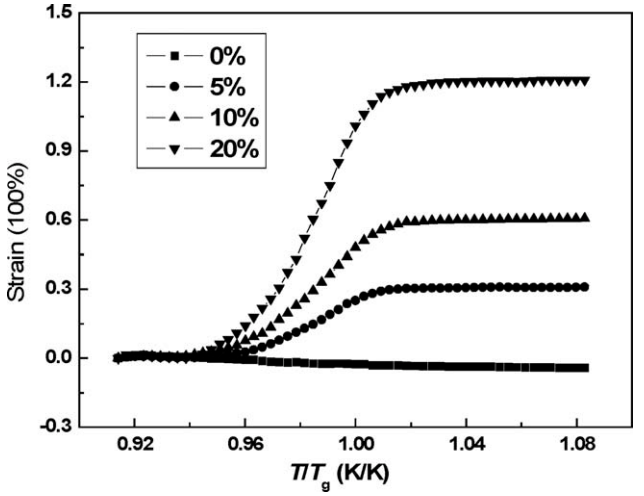

Figure 8 Strain-constraint recovery responses during the heating process.

neither the same nor symmetric with T_g. It is much lower than T_g during the cooling process, but very close to T_g during the heating process. It should be pointed out that the above result is very important in considering thermomechanical constitutive equations of SMPs. To simulate the frozen and recovery responses of SMPs under different conditions, various thermomechancial models were ever proposed.[27–29] In these models, a parameter called frozen fraction Φ_f was commonly defined. Although different expressions of Φ_f were considered, they could be uniformly expressed as

$$\Phi_f = F\left(\frac{T}{T_{\text{tran}}}\right) \tag{1}$$

If T_{tran} is not a material's parameter, and the values during the heating and cooling processes are different, the expression of the frozen fraction in eq. (1) cannot effectively simulate the frozen and recovery responses of SMPs simultaneously.

According to the testing results, viscoelastic characteristics of SMPs might cause T_{tran} apart from T_g and further affect the shape frozen and recovery responses. In addition, the results also confirm that

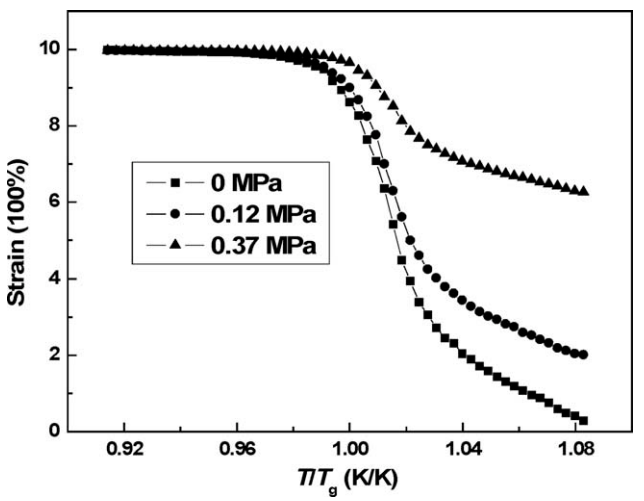

Figure 9 Stress-constraint recovery responses during the heating process.

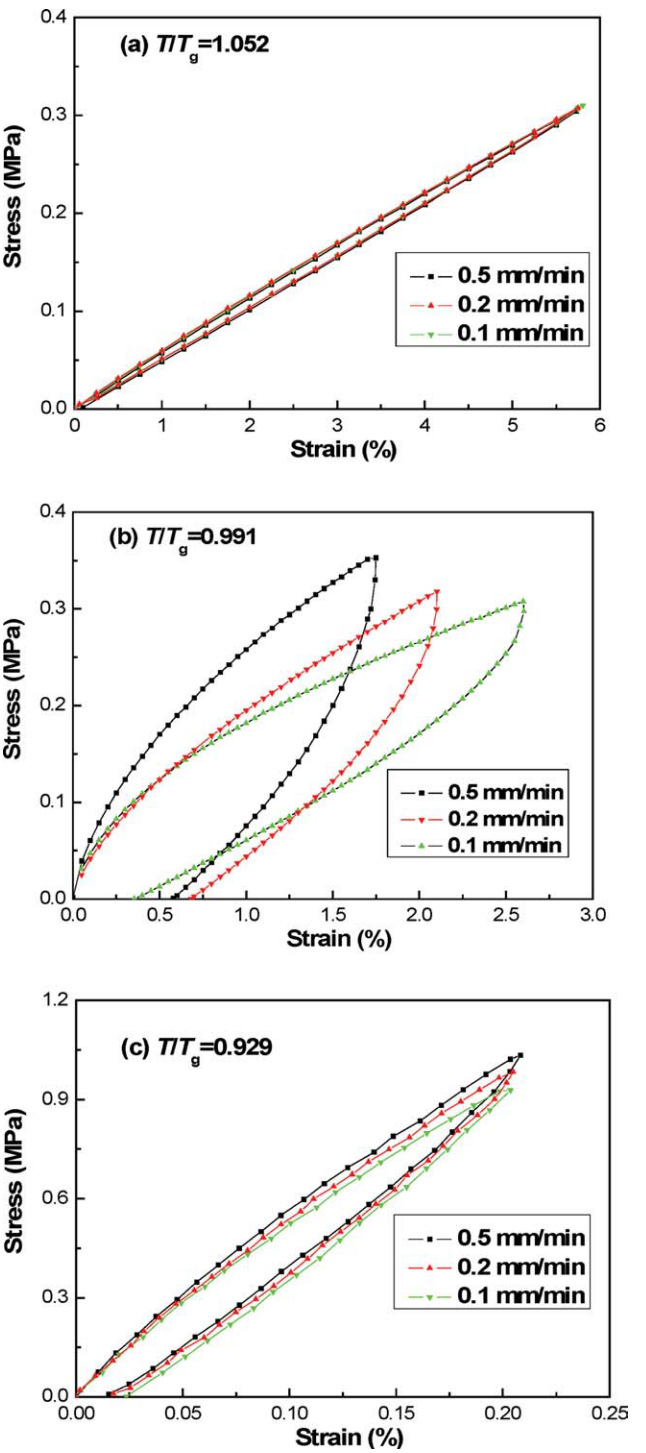

Figure 10 Stress-strain hysteresis at different temperatures. [Color figure can be viewed in the online issue, which is available at www.interscience.wiley.com.]

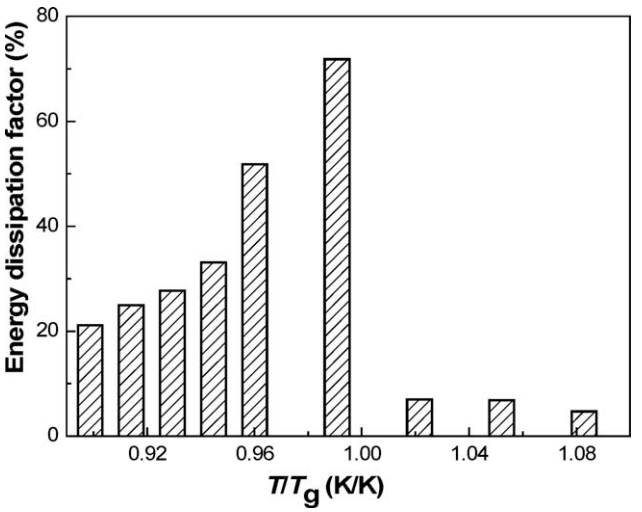

Figure 11 Energy dissipation factors at different temperatures.

the viscoelastic effect in glassy state seems to be different from that in rubbery state. To get a better understanding of the viscoelastic characteristics, experiments of stress-strain hysteresis and stress relaxation at different temperatures were performed. The results will be reported in the following sections.

Stress-strain hysteresis

Figure 10 presents the testing results of the stress-strain hysteresis of shape memory polyurethane at different temperatures. In rubbery state, a nearly linear elastic response appears [Fig. 10(a)]. Hence, as the thermomechanical experimental results of the shape recovery process shown in the above, no significant time-delay appears. The recovery strain increases very quickly and soon reaches to the saturation value when the temperature is higher than T_g. The significant viscoelastic response appears at the temperature which is very close to T_g [Fig. 10(b)]. With further decreasing of the temperature [Fig. 10(c)], the viscoelastic behavior is reduced, but still higher than that in rubbery state. Consequently, the switching transition temperature during the cooling process is much lower than T_g as presented in the former Section 2.3.

The enclosed area of the stress-strain hysteresis in Figure 10 reflects the energy dissipation, while the residual strain after a stress-strain loop reflects the creep behavior of the material. In this study, two viscoelastic factors, η_1 and η_2, are respectively defined as

$$\eta_1 = \frac{E_{\text{Loss}}}{E_{\text{Elastic}}}, \quad \eta_2 = \frac{\varepsilon_{\text{creep}}}{\varepsilon_{\max}} \tag{2}$$

where E_{Loss} and E_{Elastic} denote the loss energy and elastic energy in the stress-strain hysteresis, respectively; and $\varepsilon_{\text{creep}}$ and $\varepsilon_{\max}$ represent the creep strain and the maximum strain in the stress-strain hysteresis, respectively. Figures 11 and 12, respectively, show the testing results of energy dissipation factor η_1 and creep factors η_2 at different temperatures, which are received with the displacement control of 0.2 mm/min. It is clear that the variations of η_1 and η_2 affected by the temperature are very similar with that of the loss modulus as shown in Figure 5. Both η_1 and η_2 reaches the maximum values at temperatures close to T_g. With the decreasing of temperatures, both η_1 and η_2 will reduce, but change very slowly. However, when increasing the temperature above T_g, both η_1 and η_2 decrease very quickly. The results indicate that the viscoelastic behavior of SMPs is not symmetric with T_g, and its effect at low temperature is more serious than that at high temperature, which can give a reasonable explanation why T_{tran}-values of SMPs are different in frozen and recovery processes.

Stress relaxation

In addition to the stress-strain hysteresis, stress relaxations of the material at different temperatures were also investigated experimentally. Figure 13 presents some typical testing results. In agreement with the stress-strain hysteresis testing results, stress relaxation ratio (the relaxed stress divided by the prestress) of shape memory polyurethane in glassy state is higher than that in rubbery state, and it reaches the maximum value when the temperature is close to T_g. Similarly, the following stress relaxation factor is defined:

$$\eta_3 = \frac{\sigma_R(t)}{\sigma_{\text{pre}}} \tag{3}$$

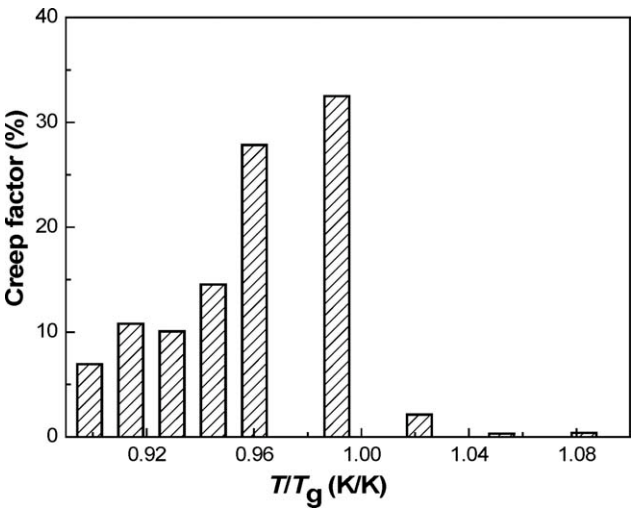

Figure 12 Creep factors at different temperatures.

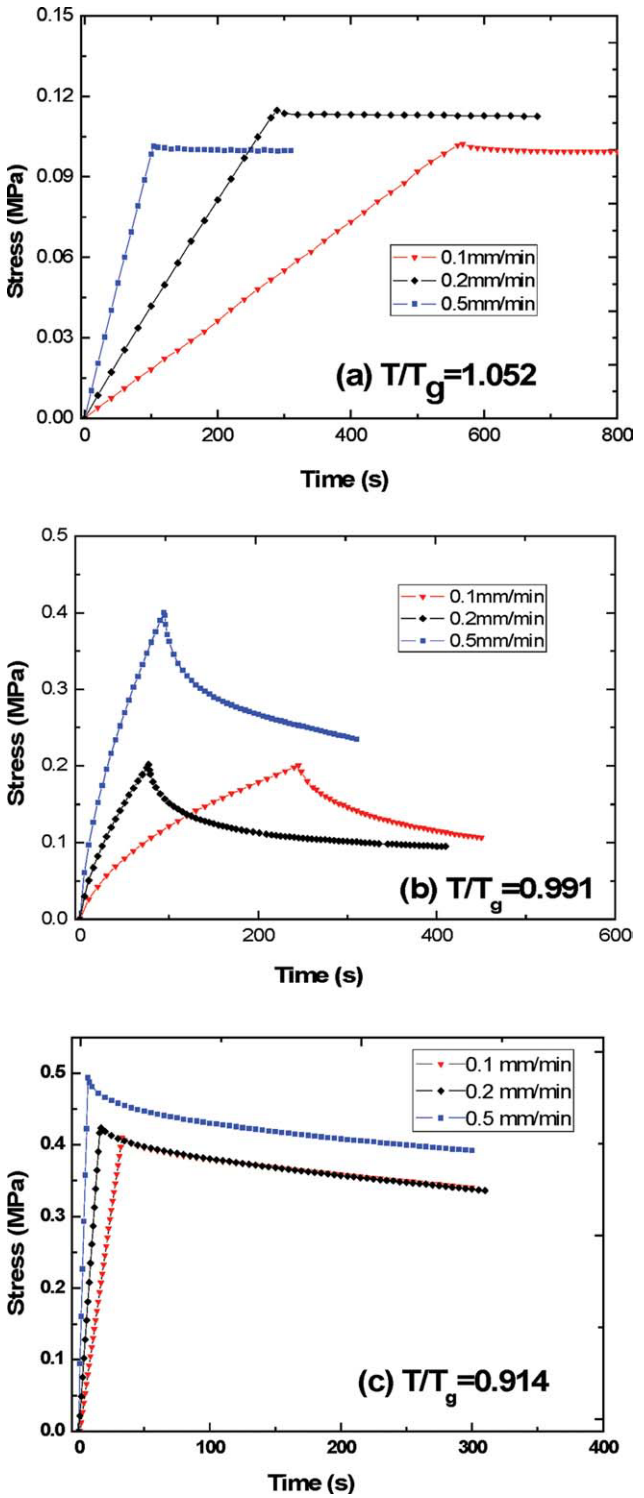

Figure 13 Stress relaxation of shape memory polyurethane at different temperatures. [Color figure can be viewed in the online issue, which is available at www.interscience.wiley.com.]

where σ_{pre} denotes the prestress; $\sigma_r(t)$ represents the relaxed stress and is a function of the loading time. Figure 14 shows the results at different temperatures when the relaxed time is 200 s, which is very similar with the changing tendency of η_1 and η_2 (see Figs. 11 and 12).

CONCLUSIONS

The shape frozen and recovery responses, stress-strain hysteresis, and stress-relaxation of shape memory polyurethane were experimentally researched. The effects of the viscoelastic characteristics on the shape storage and recovery responses of the material were considered. Some discussions are presented on the relations between T_{tran} and T_g. Consequently, the following results were obtained:

a. Approximately linear relations of CTE versus temperatures are received for shape memory polyurethane both in glassy and rubbery states. However, a significant increase of CTE-values appears from glassy state to rubbery one. The curve of CTE versus temperatures clearly reflects the different micro-structure characteristics of the material in glassy and rubbery states.
b. Thermomechanical experiments confirm that T_{tran} is different from T_g. During the shape frozen process, T_{tran} is much lower than T_g, but they have no significant difference during the shape recovery process. This is due to the different viscoelastic characteristics of SMPs at the temperatures above and below T_g.
c. The experimental results of stress-strain hysteresis and stress relaxation show that the viscoelastic effect of SMPs reaches to a maximum value at T_g. Then it decreases slowly with decreasing temperatures and reduces much quickly with increasing temperatures. The result can provide a reasonable explanation

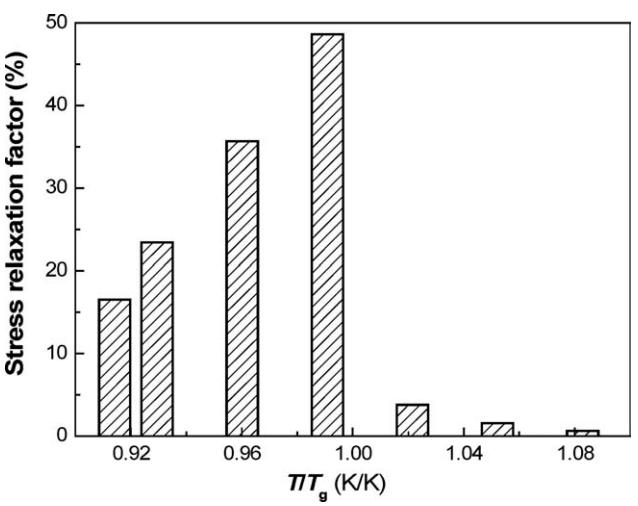

Figure 14 Stress relaxation factor affected at different temperatures.

about the frozen and recovery responses of SMPs under different constraint conditions.

References

1. Wei, Z. G.; Sandrom, R. J Mater Sci 1998, 33, 3743.
2. Ota, S. Rad Phys Chem 1981, 18, 81.
3. Robin, J.; Martinot, S.; Curtil, A.; Vedrinne, C.; Tronc, F. J Thorac Cardiovasc Surg 1998, 115, 898.
4. Feninat, F. E.; Laroche, G.; Fiset, M.; Mantovani, D. Adv Eng Mater 2002, 4, 91.
5. Lendlein, A.; Langer, R. Science 2002, 296, 1673.
6. Campbell, D.; Lake, M. S.; Scherbarth, M. R.; Mallick, K. Presented at the 46th Structural Dynamics, and Materials Conference, Austin, Texas, 2005.
7. Tupper, M.; Gall, K.; Mikulas, M. IEEE 2001, 5, 2541.
8. Lake, M. S.; Munshi, N. A.; Tupper, M. L. AIAA Journal Paper No. 2001-4602.
9. Kane, R. S.; Takayama, S.; Ostuni, E. D.; Ingber, D. E. Biomater 1999, 20, 2363.
10. Jackson, W. C.; Tran, H. D.; O'brien, M. J.; Rabinovich, E. Lopez, G. P. J Vac Sci Tech 2001, 19, 596.
11. Gall, K.; Kreiner, P.; Turner, D.; Hulse, M. J Microelectrome 2004, 13, 472.
12. Yang, B.; Huang, W. M.; Li, C. Presented at the 1st International Symposium of Nanotechnology, Singapore, **July** 13–17, 2004.
13. Yang, B.; Huang, W. M.; Li, C.; Chan, Y. S. Eur Polym J 2005, 41, 1123.
14. Kim, B. K.; Lee, S. Y. Polymer 1996, 37, 5781.
15. Gall, K.; Mikulas, M.; Munshi, N. A.; Beavers, F.; Tupper, M. J Intell Mater Syst Struct 2000, 11, 877.
16. Jeong, H. M.; Lee, S. Y.; Kim, B. K. J Mater Sci 2000, 35, 1579.
17. Beloshenko, V. A.; Beygelzimer, Y. E.; Borzenko, A. P.; Varyukhin, V. N. Compos Part A 2002, 33, 1001.
18. Liu, C. D.; Chun, S. B.; Mather, P. T.; L.; Haley, R.; Coughlin, R. B. Macromolecules 2002, 35, 9868.
19. Metcalfe, A.; Desfaits, A. C.; Salazkin, I.; Gilmartin, K.; Embry, G.; Boock, R. J. Biomaterials 2003, 24, 491.
20. Jeong, H. M.; Lee, S. Y. Eur Polym J 2004, 40, 1343.
21. Lendlein, A.; Kelch, S. Angew Chem Int 2002, 41, 2034.
22. Tobushi, H.; Hara, H.; Yamada, E.; Hayashi, S. Smart Mater Struct 1996, 5, 483.
23. Tobushi, H.; Okumura, K.; Hashimoto, T.; Hayashi, S.; Ito, N. Mech Mater 2001, 33, 545.
24. Rao, I. J. In Proceedings of SPE-ANTEC; Sanfrancisco, CA, 2002; 1785.
25. Rao, I. J.; Rajagopal, K. R. Int J Solids Struct 2001, 38, 1149.
26. Abrahamson, E. R.; Lake, M. S.; Munshi, N. A.; Gall, K. J Intell Mater Syst Struct 2003, 14, 623.
27. Liu, Y. P.; Gall, K.; Dunn, M. L.; Greenberg, A. R.; Diani, J. Int J Plasticity 2006, 22, 279.
28. Chen, Y. C.; Lagoudas, D. C. J Mech Phys Solids 2008, 56, 1766.
29. Wang, Z. D.; Li, Z. F.; Xiong, Z. Y.; Chang, R. N. Appl Polym Sci 2009, 113, 651.
30. Metzger, M. F.; Wilson, T. S.; Schumann, D. Biomed Microdevices 2002, 4, 89.
31. Gall, K.; Dunn, M. L.; Liu, Y. P.; Finch, D.; Lake, M.; Munshi, N. A. Acta Mater 2002, 50, 5115.